Studying the effect of copper on the p-ZnTe/n-AgCuInSe$_2$/p-Si for thin films solar cell applications

R. H. Athab, B. H. Hussein[*]
Department of physics, College of Education for Pure Science / Ibn Al-Haitham, University of Baghdad, Baghdad, Iraq

A thin film of AgInSe2 and Ag$_{1-x}$Cu$_x$InSe$_2$ as well as n-Ag$_{1-x}$Cu$_x$InSe$_2$ /p-Si heterojunction with different Cu ratios (0, 0.1, 0.2) has been successfully fabricated by thermal evaporation method as absorbent layer with thickness about 700 nm and ZnTe as window layer with thickness about 100 nm. We made a multi-layer of p-ZnTe/n-AgCuInSe2/p-Si structures, In the present work, the conversion efficiency (η) increased when added the Cu and when used p-ZnTe as a window layer (WL) the bandgap energy of the direct transition decreases from 1.75 eV (Cu=0.0) to 1.48 eV (Cu=0.2 nm) and the bandgap energy for ZnTe=2.35 eV. The measurements of the electrical properties for prepared films showed that the D.C electrical conductivity (σ$_{d.c}$) increased with increasing Cu content for AgCuInSe2 thin films. So the electrical conductivity changed from 1 (Ω.cm)$^{-1}$ to 29.96 (Ω.cm)$^{-1}$ when x changed from 0.0 to 0.2. The prepared thin films have two activation energies (E$_{a1}$ & E$_{a2}$) in the temperature ranges of (300-393) K and (303-473) K. The C-V measurements revealed that all prepared heterojunctions were of the abrupt type and the junction capacitance reduced while the width of depletion region and the built-in potential increased with increasing the Cooper content. The current-voltage characteristics under dark condition of AgCuInSe2 heterojunctions, the current-voltage measurements under illumination showed that the performance of heterojunction solar cell improved with increasing Cu content. The result indicated that the prepared solar cell with 0.2 Ag content exhibited the highest efficiency (η = 1.68%) compared to other prepared solar cells.

1. Introduction

Thin film development of solar cell make use of at least two types of semiconductor layers the first a narrow bandgap absorber material and the second-wide bandgap window material. The most research absorber materials are CuInGaSe2 and CdTe, two cases the majority of researchers used a n-CdS layers as a window material[1] The use of wide bandgap windows (p-type) material instead of n-type layer as products higher potential barrier for electron passage, lead to high Voc value. The employ of ZnTe as a window layers can also decrease the toxic nature by replacing CdS layer used in thin films solar cell [2,3] Electrodeposit ZnTe layer using a nonaqueous mediums of ethylene glycol (EG), in order to use these layer in thin film solar cells based on CdTe[4] In recent years, AgInSe2 has received much attraction for photovoltaic energy conversion [5] Therefore, it is essential to understand the optical losses for the decrease conversion efficiency of the AgInSe2-based solar cell [4,6]. The I–III–VI2 semiconductor materials have global energy and environmental problems. It is founded to be candidate material for low cost solar cell absorber [7]. high absorption, and chemical flexibility that allows for the alteration of the bandgap and between 1.07 and 2.73 eV cover the entire solar spectrum which makes it an ideal system for multi junction solar cell [8] the crystal structure is tetragonal structure chalcopyrite with the lattice constant a =b= 6.102 A° and c = 11.69 A° of AgInSe2 [9]. While ZnTe are with wide energy band-gap (2.26-2.4) eV [10,11,12] the crystal structure is Cubic structure chalcopyrite with the lattice constant a = 6.101 Å [13]. AgInSe2 exhibit n-type conductivity [5] Where ZnTe can be used as a p-type conductivity [4,14].

In order to recognize the AgInSe2 -based photovoltaic device it is necessary to realize the effect of WL on the absorber layers in the heterojunction structures. In the present study fabrication of multi-layer heterojunction structure of p-ZnTe/n-AgCuInSe2/p-Si for solar cell applications was manufactured by vacuum evaporation method.

2. Experimental

In this study, heterojunction multi-layer structures of p-ZnTe/n-AgCuInSe2/p-Si where p-ZnTe as a window layer with thickness about 100 nm and n-$Ag_{1-x}Cu_xInSe_2$ as absorbent layer with thickness about 700 nm, the Silver Ag, Copper Cu, Indium In and selenium Se elements stoichiometric proportions with different Cu ratios (0, 0.1, 0.2) and Zinc Zn, Telluride Te as shown in Figure (1).
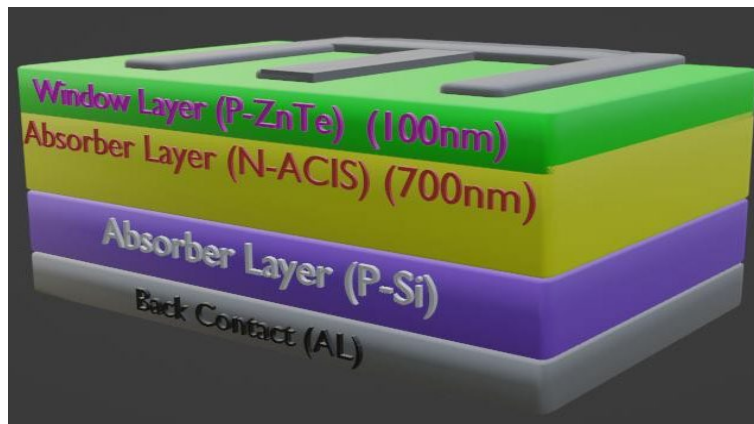

Fig. 1. Schematic represent the Al/ p-ZnTe/n-AgCuInSe2/p-Si /Al HJs solar cells.

The AgCuInSe2 thin films were prepared by using (E 306) thermal evaporation at RT deposited on glass substrates at R.T for study the electrical, structural, and optical properties of ACIS thin film. The ratios of the elements used for preparing ACIS alloys with different Cu content were verified using Energy Dispersive X-ray Spectrometer (EDS) of type (XFLASH6L10) from the (Bruker company, Germany).

Optical properties of thin film prepare, Tauc equation and lambert law have been used to determine the absorption coefficient α and the energy gap (Egopt) respectively from absorption spectrum [15,16] dielectric loss (tan δ) and optical conductivity (б) [17]:

$$\alpha h\upsilon = D (h\upsilon - E_g)^r \tag{1}$$

$$\alpha = 2.303 \frac{A}{t} \tag{2}$$

$$б = \alpha nc \tag{3}$$

$$\tan \delta = \varepsilon_i / \varepsilon_r \tag{4}$$

α: absorption coefficient, hv the incident photon energy, r: a parameter for the type of the optical transition. A: absorbance, t: thickness D is a constant depends on the temperature and the properties of the valence & conduction bands, real part ε_r & imaginary part ε_i of dielectric constant, n refractive index, c light's velocity.

Electrical Measurements, D.C Conductivity, the equation gives the relation between the electrical conductivity and temperature is called Arrhenius equation [18]:

$$\sigma_{d.c} = \sigma_o \exp(-E_a/k_B T) \tag{5}$$

where σ_o is the minimum electrical conductivity, E_a the activation energy, k_B is Boltzmann constant and T is the absolute temperature.

The depletion width w and capacitance C can be obtained by solving Poisson equation. Anderson assumed in this model that the diffusion current consists almost entirely of holes or electrons due to band edges discontinuity [19].

$$C = [\frac{qN_{D1}N_{A2}\varepsilon_1\varepsilon_2}{2(\varepsilon_1 N_{D1} + \varepsilon_1 N_{A2})(V_{bI} - V)}]^{\frac{1}{2}} \tag{6}$$

where ε_n & ε_p are the permittivity of n and p–type semiconductors, respectively, N_a & N_d are the acceptor and donor concentrations, correspondingly, V_{bi} is junction built–in potential and V is applied voltage in reverse bias.

The equations that describe the Current – Voltage properties under illumination and dark are [20]:

$$I = I_s \left\{ \exp\left(\frac{qV}{\beta k_B T}\right) - 1 \right\} - I_L \tag{7}$$

Fill factors is well-defined as the ratio between the maximum power obtained from the solar cell (P_{max}) and the product of I_{sc} and V_{oc}. F.F can be represented by the following relation [21]:

$$F.F. = \frac{P_{max}}{V_{oc}J_{sc}} = \frac{V_{max}I_{max}}{V_{oc}I_{sc}} \tag{8}$$

where I_{max} and V_{max} are current and voltage parallel to the P_{max}.

The conversion efficiency which represents the ratio between the solar cell maximum power and incident light power (P_{in}). The conversion efficiency of the solar cell is given by [21]:

$$efficiency = \eta = \frac{P_{max}}{P_{in}} * 100\% = \frac{F.F\, V_{oc}\, I_{sc}}{P_{in}} * 100\% \tag{9}$$

3. Results and discussion

The presence of dopants and the composition of samples are confirmed through EDXA measurements The compositional analysis by EDXA measurements on AgInSe2 samples gives an atomic percentage of films with different Cu ratios (0, 0.1, 0.2) are depicted in Figure (2) and Table (1). EDAX measurements on ZnTe sample displays in Figure (3) and Table (2).

Table 1. The composition of $Ag_{1-x}\,Cu_x In\,Se_2$ determined by (EDS).

samples	Theoretical concentration of elements%				Experimental concentration of elements%			
	Ag	Cu	In	Se	Ag	Cu	In	Se
AgInSe$_2$	28.341	0	30.167	41.491	28.342	0	30.168	41.490
Ag$_{0.9}$Cu$_{0.1}$In Se2	25.807	1.689	30.522	41.980	25.805	1.688	30.521	41.983
Ag$_{0.8}$Cu$_{0.2}$In Se2	23.214	3.418	30.885	42.482	23.215	3.419	30.887	42.483

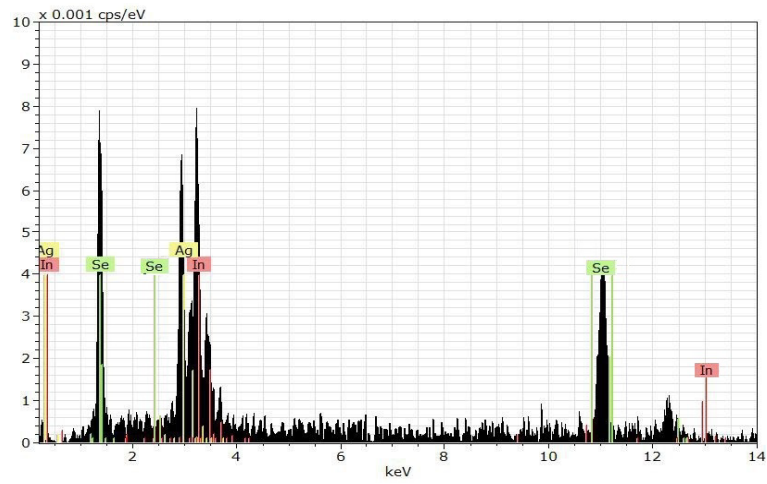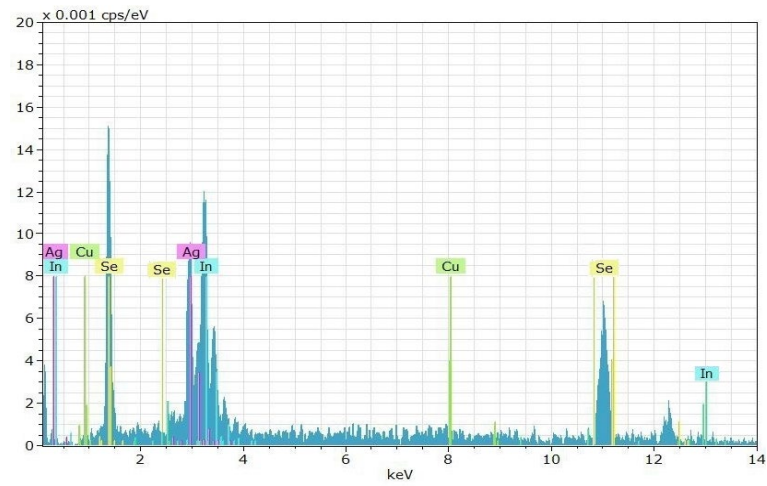*Fig. 2. (a). EDAX spectra of a typical AgInSe2 thin film.*

Fig. 2. (b). EDAX spectra of a typical AgInSe2 thin film with Cu ratio (0.1).
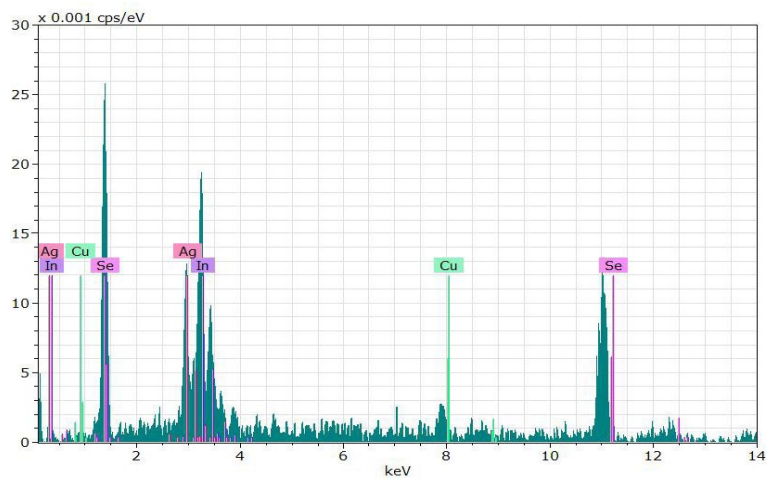

Fig. 2 (c). EDAX spectra of a typical AgInSe2 thin film with Cu ratio (0.2).
Table 2. The composition of ZnTe (EDS).

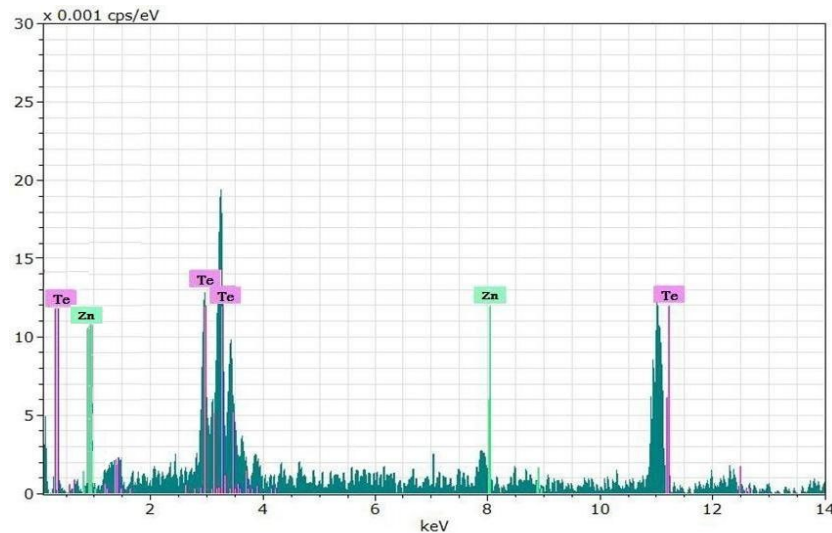| Element	Experimental concentration of elements%	Theoretical concentration of elements%
Zn	33.872	33.871
Te	66.121	66.131

Fig. 3. EDAX spectra of a typical of ZnTe thin film.

The optical energy band gap E_g^{opt} *of* varies Cu ratios can be calculated using the Tauc Equation 1. Figure (4a,b) illustrates the relationship of $(\alpha h\upsilon)^2$ on the vertical axis with $h\upsilon$ on the horizontal axis of different Cu ratios of $Ag_{1-x}Cu_xIn\ Se_2$ as absorbent layer and ZnTe as window layer. The value of the gap energy of $Ag_{1-x}\ Cu_xIn\ Se_2$ /glass film decreases (1.75, 1.68 and 1.48) eV as the Cu ratios increases (0, 0.1 and 0.2).Various information have been published to explain that the bandgap decreases with the increase of the Cu ratios[22,23], is attributed to structural & microstructural parameter e.g. addition in particle size, The value of the gap energy of ZnTe as window layer was 2.35 eV [10, 11 and 12] as in Figure (4a,b) and Table 3. Difference of dielectric loss (tan δ) and optical conductivity (б) function for $Ag_{1-x}\ Cu_xIn\ Se_2$ /glass thin film is show in Figure 5 and Table 3. It is clear that dielectric loss function depended on real part ε_r & imaginary part ε_i of dielectric constant and decreases with increasing wavelength and it has maximum value equals to 0.3 at 450 nm wavelength. The optical conductivity of $Ag_{1-x}Cu_xIn\ Se_2$ /glass depended on the absorption coefficient, n refractive index, c light's velocity of thin films is also decreases with wavelength and high value in $18*10^{12}$.

Table 3. Optical parameters (E_g^{opt}, α, tan δ, and б) for $Ag_{1-x}Cu_xIn\ Se_2$ samples with different Cu ratios (0, 0.1, 0.2) film where λ=500nm.

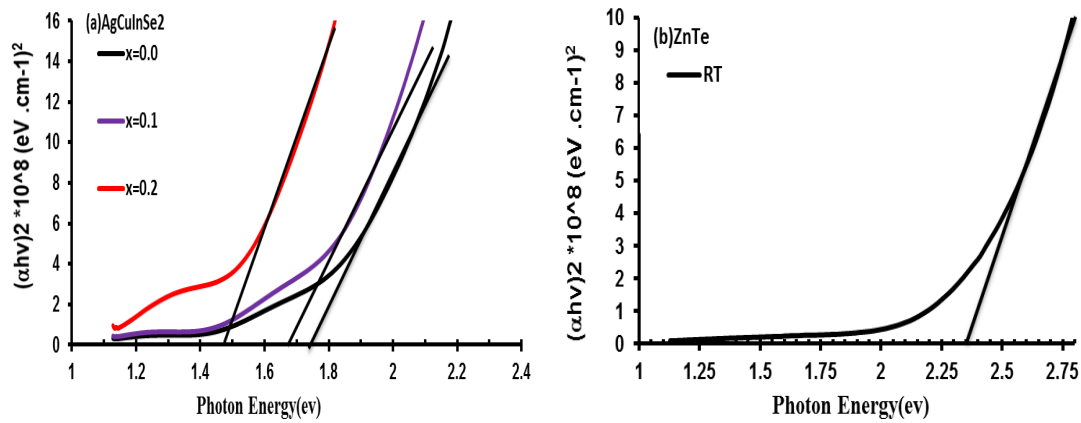| Thin films	E_g^{opt} (eV)	$\alpha \times 10^4$ cm^{-1}	tan δ	б*10^12
Cu(0.0)	1.75	2.5	0.12	14.2
Cu(0.1)	1.68	3.1	0.14	15.8
Cu(0.2)	1.48	3.8	0.19	17.6

Fig. 4. The $(\alpha h\nu)^2$ with photon energy E_g for (a) AgInSe2 samples with different Cu ratios (0, 0.1, 0.2), (b) ZnTe.
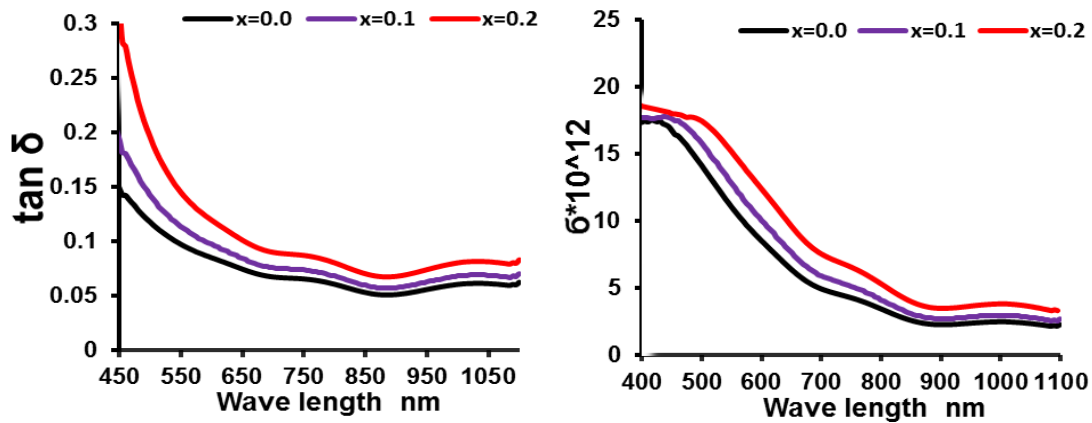

Fig. 5. Variation of dielectric loss function and optical conductivity for AgInSe2 samples with different Cu ratios (0, 0.1, 0.2).

From Figure (6), it is observed that the conductivity for all prepared $Ag_{1-x}Cu_xIn Se_2$ thin films increases with increasing temperature in the range (300-473) K, this means that all films have a negative thermal coefficient with resistivity and this is a property of semiconductors [18,24]. It can be concluded that there are two mechanisms of the conductivity giving increase to the two activation energies E_{a1} and E_{a2}, the first activation energy happens at lower temperature within the range (300-393)K, and the second activation energy happens at higher temperature within the range (403-473)K. It is clear from Table (4) when the Cu ratios increases (0, 0.1 and 0.2), the two activation energies are decreased and thus the thin film conductivity increases. The same behavior was observed by Rajani Jacob *et. al* [18].

Table 4. Electrical parameters from D.C conductivity measurement for $Ag_{1-x}Cu_xIn Se_2$ thin film with different Cu content.

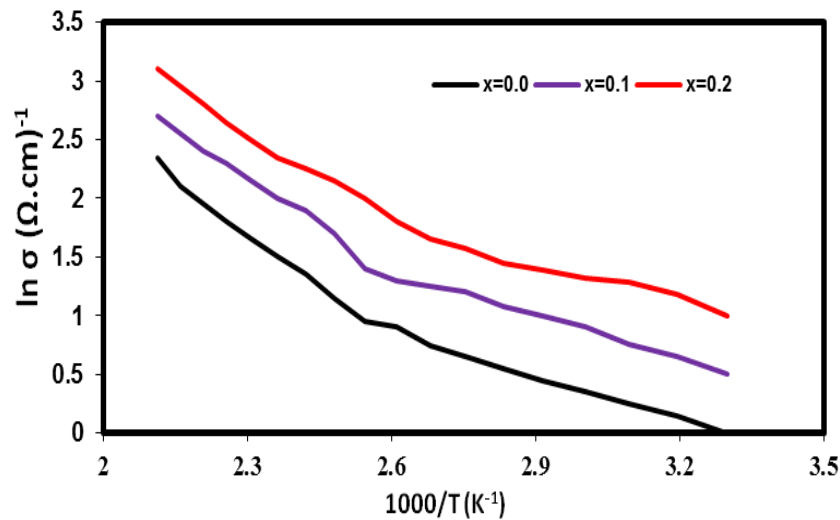| x	$\sigma_{R.T}$ $(\Omega.cm)^{-1}$	E_{a1} (eV)	Temp. Range (K)	E_{a2} (eV)	Temp. Range (K)
0.0	1.00	0.107	300-393	0.2659	403-473
0.1	7.5	0.067	300-393	0.1892	403-473
0.2	29.96	0.028	300-393	0.164	403-473

Fig. 6. lnσ vs. (1000/T) for as deposited and annealed Ag$_{1-x}$Cu$_x$In Se$_2$ thin films with different Cu content.

Electrical properties contain the capacitance-voltage (C-V) and the current-voltage (I-V) characteristics measurements for Al/n-Ag$_{1-x}$Cu$_x$In Se$_2$ /p-Si (111)/Al heterojunctions fabricated at RT with different Cu content (0.0, 0.1 and 0.2). C-V measurement is considered a key aspect for studying the electrical properties for ACIS HJs. It is a very important method for determining the type, built-in potential (V$_{bi}$), depletion region width (W), zero bias capacitance (C$_o$) and carrier concentration (N$_p$) of heterojunction.

Figure (7) presents the relation between inverse capacitance squared for all the prepared heterojunctions as with of the reverse bias voltage. The linearity of 1/C^2-V characteristics indicates that the junction is an abrupt [19,20]. From the intercept of the straight line through x-axis and y-axis, the values of V$_{bi}$ and C$_o$, were obtained, respectively while the carrier concentration was deduced from the slope of the straight line. Finally, the depletion region width was calculated. The obtained results are listed in Table (5). It is clear that the increases in Cu content led to a decrease in the carrier concentration, which in turn decrease the zero bias capacitance and increase the value of the built-in potential and the depletion region width. A thicker depletion region is preferred to separate photogenerated e-h pairs but causes high resistivity [25].

Table 5. C-V measurement Parameters for Al/(Ag$_{1-x}$Cu$_x$In Se$_2$) /Si/Al heterojunctions with different Cu content.

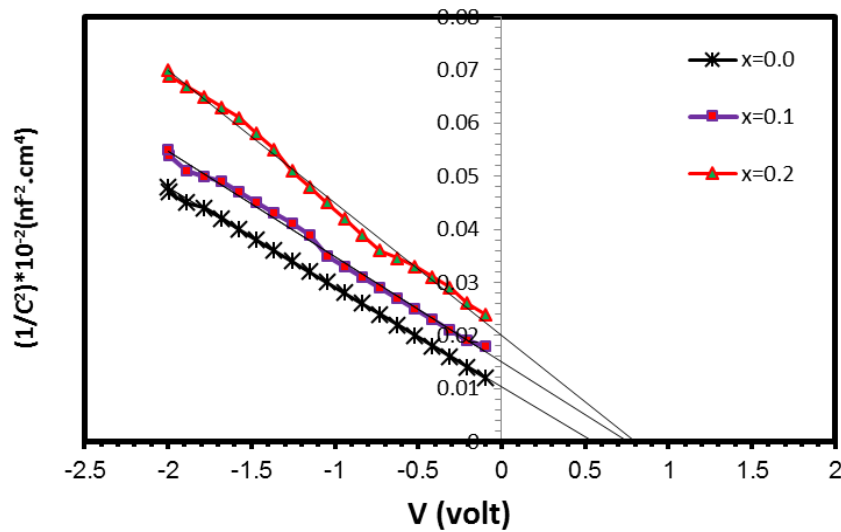| x	V$_{bi}$ (volt)	C$_o$ (nF/cm^2)	W (nm)	N$_d$*10^{16} (cm^{-3})
0	0.5	98.53292782	41.64090209	1.08
0.1	1.05	59.86843401	68.53361154	1.15
0.2	1.4	36.56362121	112.2153623	1.55

Fig. 7. 1/C² as function of applied voltage for Al/(Ag$_{1-x}$Cu$_x$In Se$_2$) /Si/Al heterojunctions with different Cu content.

Figure (8) shows the I-V characteristics curve for prepared Al/ZnTe/ Ag$_{1-x}$Cu$_x$In Se$_2$ /Si/Al HJ solar cells at RT with various Cu content (0, 0.1 and 0.2). Open circuit voltage (V$_{oc}$) and short circuit current (I$_{sc}$) are very significant parameters because they can determine the region in which the heterojunction operates. The magnitude of V$_m$ (maximum voltage) and I$_m$ (maximum current) are estimated at maximum power point on the photovoltaic power output curve as seen in Figure (7). The value of the fill factor and efficiency are calculated using Eq. (8) and (9), respectively. All obtained values are tabulated in Table (6). It is clear from Table (7) that the values of V$_{oc}$ and I$_{sc}$ are increased as x value increased which in turn increase the V$_{max}$, I$_{max}$ and the F.F. This may be attributed to the improvement in the absorber layer properties with increasing x content. It is also noticed that the photoconversion efficiency (PCE) of the cell increases with increasing x content. This may be due to increase the particle size of the absorber layer with increasing Cu content and T$_a$. The PCE of the prepared cell is strongly related to the particle size because a large particle size in the absorber layer maximizes both the minority carrier diffusion length and the built in potential. The increase in PCE can also be attributed to the increase in the width of the depletion region [26].

Table 6. Values of Jsc, Voc, Jmax, Vmax, F.F and efficiency (η %) for Al/ZnTe/ Ag$_{1-x}$Cu$_x$In Se$_2$ /Si/Al HJs solar cells with various x value.

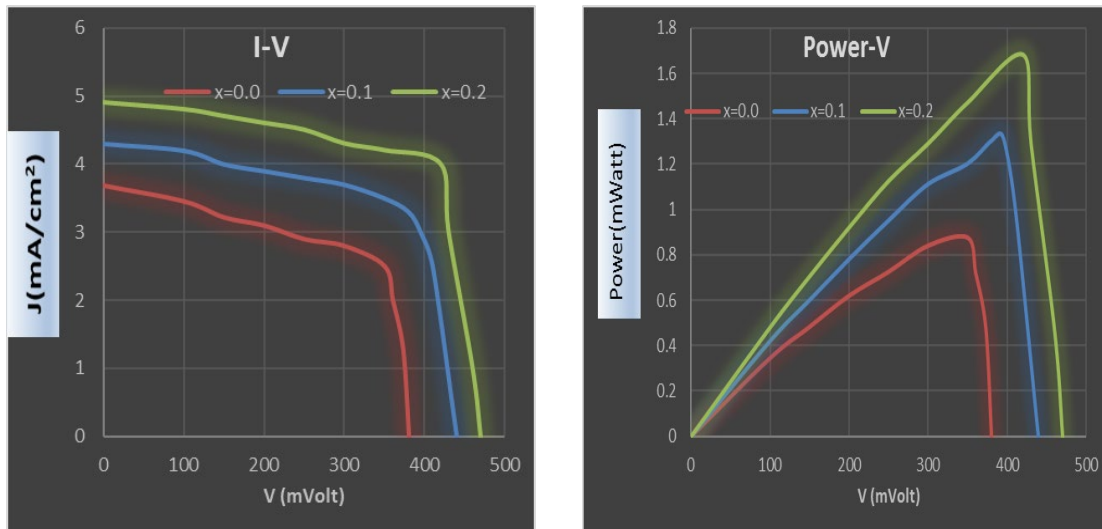| x	J$_{sc}$(mA)	V$_{oc}$(mV)	J$_{max}$(mA)	V$_{max}$(mV)	F.F	η%
0	3.68	380	2.5	350	0.625715	0.875
0.1	4.3	440	3	395	0.63	1.32
0.2	4.9	470	4	420	0.729483	1.68

Fig. 8. Isc and Voc curves Al/ZnTe/ $Ag_{1-x}Cu_xIn\ Se_2$ /Si/Al HJs solar cells with various x value.

4. Conclusions

All $Ag_{1-x}Cu_xIn\ Se_2$ thin films had a high absorbance in the visible region while all thin ZnTe films had a high transmittance in visible and infrared region. The optical transition in all ACIS and ZnTe thin film was observed to be allowed direct transition and the value of optical band gap decreased with increasing x content for ACIS films. D.C measurements showed the presence of two transport mechanisms of the charge carriers in two ranges of temperatures in both types of thin films. C-V measurements indicated that all fabricated Al/ZnTe/ Ag1-xCuxIn Se2 /Si/Al HJs were of the abrupt type and the values of the depletion region width and the built-in potential increased but the capacitance and carrier concentration values decreased with increasing x content. I-V characteristics under illumination showed that the act of the manufactured solar cell improved with increase x value. Therefore, optimum conditions in which the cell will operate for best performance (F.F=0.72 and η= 1.68%) are when x value equal to 0.2.

References

[1] Dharmadasa IM, Roberts JS, Hill G, Sol Energy Mater Sol Cell 2005;88:413-22; https://doi.org/10.1016/j.solmat.2005.05.008

[2] Mahalingam T, John VS, Rajendra S, Sebastian PJ, Semicond Sci Technol 2002;17:465-70; https://doi.org/10.1088/0268-1242/17/5/310

[3] Ishizaki T, Ohtomo T, Fuwa A., J Phys D: Appl Phys 2004;37:255-60; https://doi.org/10.1088/0022-3727/37/2/014

[4] A.B.M.O. Islam, N.B. Chaure, J. Wellings, G. Tolan, I.M. Dharmadasa, Materials Characterization 60 (2009) 160-163.

[5] S. N. Sobhi, B. H. Hussein, Journal of Ovonic Research Vol. 18, No. 4, July - August 2022, p. 519 – 526; https://doi.org/10.15251/JOR.2022.184.519

[6] Mulu Alemayehu Abate, Jia-Yaw Chang, Solar Energy Materials and Solar Cells 182 (2018) 37-44; https://doi.org/10.1016/j.solmat.2018.03.008

[7] P. Prabukanthan, M. Sreedhar, J. Meena, M. Ilakiyalakshmi, S. Venkatesan, G. Harichandran, A. Vilvanathaprabu, and P. Seenuvasakumaran, J Mater Sci: Mater Electron 32 6855-6865 (2021); https://doi.org/10.1007/s10854-021-05390-y

[8] Angel R. Aquino, Angus Rockett, Scott A. Little, and Sylvain Marsillac, IEEE, 003586 - 003590 (2011)

[9] Qian Cheng, Xihong Peng, and Candace K. Chan, ChemSusChem, 2013, 6, 102 – 109; https://doi.org/10.1002/cssc.201200588

[10] Samir A. Maki, Hanan K. Hassun, Ibn Al-Haitham J. for Pure & Appl. Sci. Vol.29 (2) (2016).

[11] A.B.M.O. Islam, N.B. Chaure, J. Wellings, G. Tolan, I.M. Dharmadasa, Mater. Charact, 60, (2009) 160 – 163; https://doi.org/10.1016/j.matchar.2008.07.009

[12] J. R. Rathod, H. S. Patel, K. D. Patel, V. M. Pathak, AIP Conference Proceedings 1393, 121 (2011); https://doi.org/10.1063/1.3653639

[13] Bushra H. Hussein, Hanan K. Hassun, NeuroQuantology, 18(5) (2020) 77-82; https://doi.org/10.14704/nq.2020.18.5.NQ20171

[14] Dumitru Manica, Vlad-Andrei Antohe , Antoniu Moldovan, Rovena Pascu, Sorina Iftimie, Lucian Ion, Mirela Petruta Suchea and Stefan Antohe, nanomaterials, 11, 2286 (2021); https://doi.org/10.3390/nano11092286

[15] Bushra H. Hussein, Iman Hameed Khudayer, Mohammed Hamid Mustafa, Auday H. Shaban, An International Journal (PIE), 2019, 13, 2, 173-186; https://doi.org/10.1504/PIE.2019.099358

[16] S. N. Sobhi, B. H. Hussein, Chalcogenide Letters Vol. 19, No. 6, June 2022, p. 409 – 416; https://doi.org/10.15251/CL.2022.196.409

[17] T. Mahalingam, V. Dhanasekaran, K. Sundaram, A. Kathalingam and J.-K. Rhee, Ionics, 18, (2012) 299-306; https://doi.org/10.1007/s11581-011-0623-6

[18] Rajani Jacob, Gunadhor S. Okram, Johns Naduvath, Sudhanshu Mallick, and Rachel Reena Philip, The Journal of Physical Chemistry C, Vol. 119, pp. 5727−5733 (2015); https://doi.org/10.1021/acs.jpcc.5b00141

[19] S.Sze and K.Ng., Physics of Semiconductor Devices, 3rd edition, John Wiley and Sons, (2007); https://doi.org/10.1002/0470068329

[20] D. A. Neamen, Semiconductor Physics and Devices, 3rd Edition , Mc Graw- Hill Com., Inc., University of New Mexico, U.S.A, (2003).

[21] Iman Hameed Khudayer, AIP Conference Proceedings,1968, pp. 030064-1- 030064-7, (2018); https://doi.org/10.1063/1.5039251

[22] Valery Gremenok, Ivan Vasiljevich Bodnar, Ignacio Mártil, Felix L Martines, S.L. Sergeev-Nekrasov and I.A. Victorov, Solid State Phenomena, 67-68, 361-366 (1999); https://doi.org/10.4028/www.scientific.net/SSP.67-68.361

[23] S. N. Sobhi, B. H. Hussein, Ibn Al-Haitham Journal for Pure and Applied Sciences, Vol. 35, No. 3, 2022, p. 16-24; https://doi.org/10.30526/35.3.2824

[24] C. Sunil H, M. Kanchan S., and M. P. Deshpande, Chinese J. of Physics, 52, 5, PP. 1588-1600, (2014).

[25] J. Henry, K. Mohanraj, and G. Sivakumar, J. Phys. Chem. C, 123, PP. 2094−2104, (2019); https://doi.org/10.1021/acs.jpcc.8b11239

[26] W. Xiaodeng, X. Jiale, and L. Chang Ming, J. Materials Chemistry A, 3, 3, PP.1235-1242, (2015); https://doi.org/10.1039/C4TA05846A